Modulating Gas Sensing Properties of CuO Nanowires through Creation of Discrete Nanosized p-n Junctions on Their Surfaces

6 AUTHORS, INCLUDING:

Kehan Yu
Nanjing University of Posts and Telecommuni…
51 PUBLICATIONS   1,626 CITATIONS

SEE PROFILE

Shumao Cui
University of Wisconsin - Milwaukee
64 PUBLICATIONS   1,511 CITATIONS

SEE PROFILE

Shun Mao
University of Wisconsin - Milwaukee
85 PUBLICATIONS   2,392 CITATIONS

SEE PROFILE

Ganhua Lu
University of Wisconsin - Milwaukee
65 PUBLICATIONS   2,642 CITATIONS

SEE PROFILE

Modulating Gas Sensing Properties of CuO Nanowires through Creation of Discrete Nanosized p−n Junctions on Their Surfaces

Mark Mashock, Kehan Yu, Shumao Cui, Shun Mao, Ganhua Lu,* and Junhong Chen*

Department of Mechanical Engineering, University of Wisconsin−Milwaukee, Milwaukee, Wisconsin 53211, United States

ⓢ *Supporting Information*

ABSTRACT: We report significant enhancement of CuO nanowire (NW) sensing performance at room temperature through the surface functionalization with SnO_2 nanocrystals (NCs). The sensitivity enhancement can be as high as ~300% for detecting 1% NH_3 diluted in air. The improved sensitivity could be attributed to the electronic interaction between p-type CuO NWs and n-type SnO_2 NCs due to the formation of nanosized p−n junctions, which are highly sensitive to the surrounding gaseous environment and could effectively manipulate local charge carrier concentration. Our results suggest that the NC-NW structure is an attractive candidate for practical sensing applications, in view of its outstanding room-temperature sensitivity, excellent dynamic properties (rapid response and quick recovery), and flexibility in modulating the sensing performance (e.g., by adjusting the coverage of SnO_2 NCs on CuO NWs and doping of SnO_2 NCs).

KEYWORDS: *nanowire, nanocrystal, p−n junction, gas sensor*
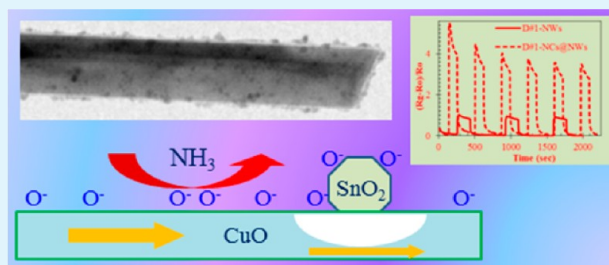
INTRODUCTION

Fast and accurate detection of trace amounts of hazardous gases is important in many aspects of human society, such as environmental monitoring and detection of toxic gases in industrial processes, public health, and national security. One-dimensional (1D) nanomaterials, such as semiconducting nanowires (NWs)[1−3] and carbon nanotubes (CNTs),[4−7] are exceedingly attractive building blocks for developing high-performance gas sensing devices, because of their outstanding physical and chemical properties (e.g., very large surface-to-volume ratios).

Surface modification or functionalization of 1D nanomaterials (e.g., NWs, CNTs) with various nanoparticles (NPs) or nanocrystals (NCs) has attracted considerable interest in gas sensing research because of promising benefits induced by the coupling and the heterointerface between the two classes of nanomaterials (i.e., 1D NWs/CNTs vs 0D NPs/NCs).[8−13] It has been reported that surface functionalization of 1D semiconducting metal oxides with catalytic metal NPs (e.g., Pd, Au, and Pt)[8,9] can further improve the sensitivity and dynamic characteristics (e.g., reduced response time). For instance, A. Kolmakov and co-workers demonstrated that the deposition of Pd NPs onto a single SnO_2 NW or nanobelt (NB) created Schottky-like junctions between the NPs and the NW/NB, resulting in electron depletion regions within the NW/NB due to electron transfer from the n-type semiconducting SnO_2 NW to the metal Pd NPs.[8] The single SnO_2 NW/NB device with Pd NP functionalization exhibited dramatically improved sensitivity toward O_2 and H_2, which is presumably because of the Pd NP-enhanced catalytic dissociation of molecular adsorbates and the consequent diffusion of resulting atomic species to the SnO_2 NW/NB surface.[8] Z. L. Wang and co-workers reported remarkably improved sensitivity of individual SnO_2 NW based gas sensing devices by surface functionalization with ZnO or NiO NPs.[10] The observed sensing enhancement was attributed to the heterojunction formed between the SnO_2 NW and NPs and the resulting coupling effect of the two sensing materials. However, those SnO_2 NW sensors, even with NP-functionalization, still required elevated temperatures (e.g., 200−270 °C[8] and 250 °C[10]) for operation.

Among metal oxides, CuO is one of very few with intrinsic p-type properties and has a low band gap of 1.2−2.0 eV.[14,15] The p-type characteristic of CuO provides a route to forming p−n junctions with n-type metal oxides, such as ZnO and SnO_2. For example, p−n junctions of this type (CuO/ZnO) have been investigated in thin-film technology to enhance gas sensing selectivity and sensitivity.[16,17] CuO NWs have been explored for gas sensing applications at elevated temperatures.[9,18,19] Previously, we have reported the room temperature sensing with individual CuO NW-based sensors.[20] This room temperature operation offers advantages for practical applications, such as reduced energy consumption by the sensor, simplified device structure (i.e., no heating element is needed), and the convenience of deploying such sensors in explosive environments where high temperature is undesirable. On the other hand, we have developed a dry technique to assemble various NCs onto CNTs[21,22] and demonstrated a room-temperature
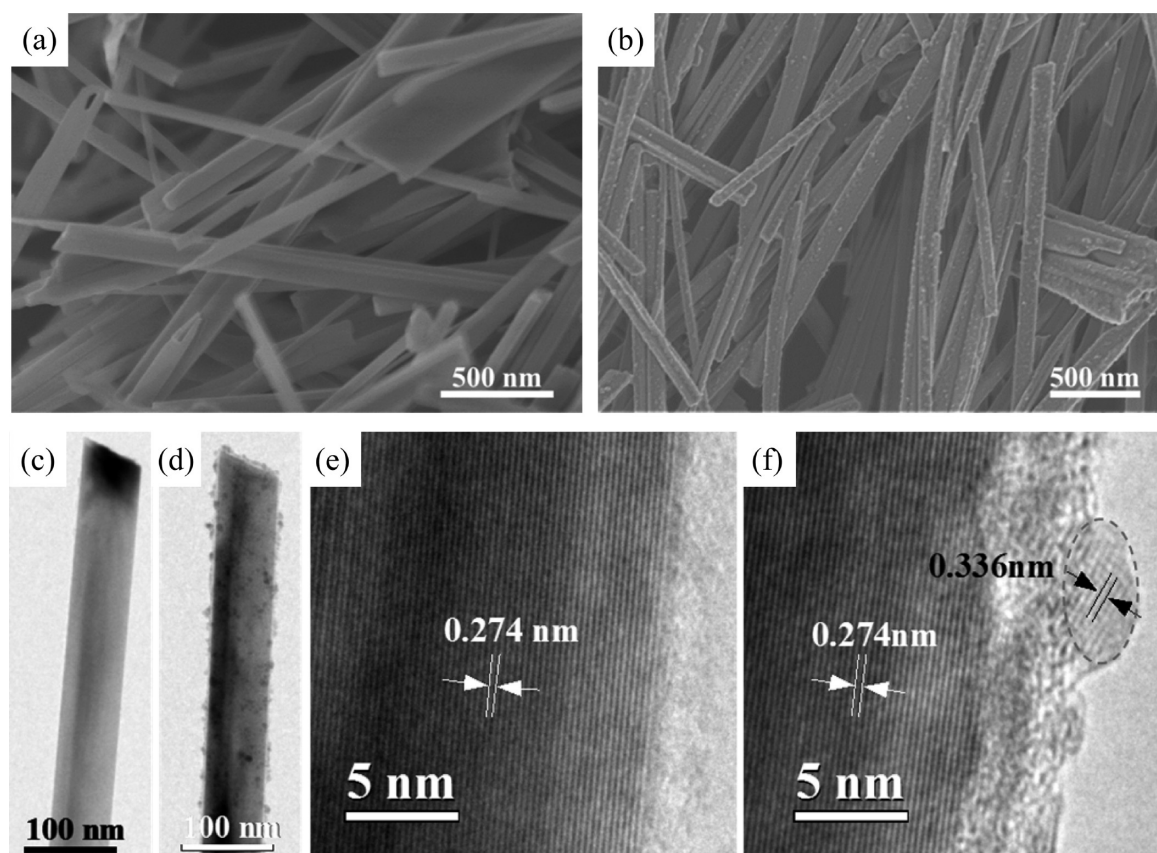
Figure 1. (a, b) SEM images of CuO NWs before and after SnO_2 coating. (c, d) TEM and (e, f) HRTEM images of an individual CuO NW (c, e) before and (d, f) after being coated with SnO_2 NCs for 3 min.

gas sensing platform consisting of multiwalled CNTs (MWCNTs) decorated with SnO_2 NCs.[23] However, MWCNTs are mostly metallic and have very high charge carrier concentration, limiting their response to electron-transfer induced perturbations. Improved sensing performance could be expected if MWCNTs are replaced with semi-conducting 1D nanomaterials (e.g., p-type CuO NWs) in the SnO_2 NC−CNT system.

In addition, a nanosized p−n junction can be formed at the interface between the p-type CuO NW (holes are majority charge carriers) and the n-type SnO_2 NC (electrons are majority charge carriers), as electrons tends to diffuse from SnO_2 to CuO while holes move from CuO to SnO_2 until an equilibrium is established at the interface.[24] The space charge region associated with the p−n junction could locally narrow the conducting channel for the charge carriers in the CuO NW, making it more sensitive to gas molecule-induced charge transfer. Here, we report on the modulation of the CuO NW electronic properties through SnO_2 NCs and the use of SnO_2 NC functionalized CuO NWs for room-temperature gas sensing. The electronic interaction between SnO_2 NCs and the CuO NWs due to the formation of p−n junctions facilitates gas detection through the change in the electrical conductivity of the hybrid NC-NW structure. In the open air, formation of oxygen adsorbates (O_2^- or O^-) on the surface of SnO_2[25] and CuO[9] results in an electron-depletion surface layer due to the electron transfer from the SnO_2/CuO to oxygen. Target gas molecules (e.g., NH_3) can react with oxygen adsorbates to free electrons back into the SnO_2/CuO surface and change electrical conductivity of the entire NC-NW structure.

■ EXPERIMENTAL DETAILS

Growth of CuO NWs on Cu Substrates. CuO NWs were synthesized by direct oxidation of copper foils.[26] The detailed procedure that we followed for CuO NW synthesis was reported previously.[20,27] Briefly, a square sample of ∼0.25 cm² was first cut from a Cu foil with 0.5 mm thickness and a purity of 99.9% (Alfa Aesar). The intrinsic oxide layer on the Cu surface was removed by ultrasonicating the sample in 0.7 M hydrochloric acid for 2 min (Hielscher Ultrasound UP 200S). The sample was ultrasonically cleaned in acetone for 5 min to remove organic contaminants, thoroughly rinsed with deionized (DI) water, and dried in compressed air.

The cleaned sample was placed directly into an open quartz tube, which was then inserted into a horizontal tube furnace (Lindberg Blue M). The furnace temperature was increased at a rate of ∼15 °C/min from room temperature to 450 °C. The sample was heated at this temperature for 2.5 h and then allowed to freely cool to room temperature. Heating in the presence of oxygen causes oxidization of Cu and the growth of CuO NWs on the sample surface.

Fabrication of CuO NW devices. An oxidized sample with CuO NWs was sonicated in a vial with methanol to detach NWs from the substrate, forming a CuO NW suspension. NWs from several samples were collected in the vial to obtain an NW suspension with a concentration sufficient for successful deposition of NWs onto interdigitated electrodes. The NW suspension was further processed in a centrifuge to separate the larger substrate particles from the NWs.

The p-doped silicon wafer covered with a 200 nm thick thermally formed SiO_2 layer was used as the device substrate, on top of which large Au contact pads (for connection with outside test equipment, e.g., a source meter) were fabricated through a standard photo-lithography process, and Au interdigitated electrodes were fabricated using an e-beam lithography process. The Au fingers (50 nm thick) of the interdigitated electrode were ∼1 μm wide and 1 μm apart. A 2 nm

thick Cr layer was used to enhance the adhesion between the Au and the Si wafer. A few drops of the CuO NW suspension were cast onto Au interdigitated electrodes, which left CuO NWs (by bottom-contact with the substrate) on the Au fingers after solvent evaporation. These NWs make the device circuit complete. As-fabricated CuO NW devices were annealed in an Ar flow at 200 °C for one hour to improve the NW-Au contact and remove remnant ethanol on NWs and on chips.

Deposition of SnO$_2$ NCs onto CuO NWs. A mini-arc plasma reactor was used to synthesize aerosol SnO$_2$ NCs (i.e., NCs suspended in gases) through physical vapor deposition.[28,29] The NCs were formed by direct vaporization of solid precursors in atmospheric direct current (dc) mini-arc plasma followed by a rapid quenching. The thermal energy from the arc discharge driven by a welding power supply (Master 150 STH) caused the solid tin powders placed in the reactor to melt and vaporize. The tin vapor was quenched by a pure and cold Ar flow to nucleate tin NCs, which were subsequently oxidized to form SnO$_2$ NCs in a pure oxygen flow. As-produced SnO$_2$ NCs were suspended in gas phase and some were electrically charged by the arc plasma or through thermionic emission.

SnO$_2$ NCs with surface charges were then deposited onto CuO NWs using an electro-static-force-directed assembly (ESFDA) technique reported before.[21,22] Briefly, in the ESFDA process, aerosol SnO$_2$ NCs were carried by room-temperature gases into a gap formed between a grounded tubing for the NC delivery and an electrically biased (−1.5 kV) substrate (e.g., the interdigitated electrode or a TEM grid) containing NWs. The electric field near the NW was significantly enhanced due to its high aspect ratio (i.e., very thin and long) and the charged SnO$_2$ NCs were attracted to the surface of oppositely charged NWs via electrostatic force. The number density of SnO$_2$ NCs on CuO NWs could be controlled by the deposition time. The ESFDA process is material independent because of the inherent nature of electrostatics force.

Sensing characterization. A sensor made of bare CuO NWs or SnO$_2$ NC functionalized CuO NWs was placed into an airtight chamber with electrical and gas feedthroughs for sensing characterization. In a sensing test, the sensor was periodically exposed to different gases while its resistance was monitored using a Keithley 2602 source meter. The sensor was operated at room temperature and periodically exposed to: clean, dry air flow (2 lpm) to record a base value of the sensor conductance for 2 or 4 min; 1% NH$_3$ diluted in air (2 lpm) to register a sensing signal for 2 or 3 min; and clean air flow (2 lpm) again to recover the device for 2 or 4 min. Multiple cycles (each of 6 or 11 min long) were performed to determine the repeatability of the fabricated sensors.

SEM and TEM characterizations. Morphologies of bare CuO NWs, SnO$_2$ NC-CuO NW structures, and fabricated sensing devices were characterized using a field-emission scanning electron microscope (SEM) (Hitachi S 4800), which has a resolution of 1.4 nm at 1 kV acceleration voltage. Morphology and crystalline structure characterizations of bare and SnO$_2$ NC-coated CuO NWs were carried out using a Hitachi H 9000 NAR transmission electron microscope (TEM) with a point resolution of 0.18 nm at 300 kV in the phase-contrast high-resolution TEM (HRTEM) imaging mode. TEM samples were prepared by adding CuO NWs onto bare Ni TEM grids (400 Mesh). To assemble SnO$_2$ NCs onto CuO NWs on a TEM grid, the ESFDA process was used. Specifically, a dc voltage of −1.5 kV was applied to the grid so that oppositely charged SnO$_2$ NCs could be attracted toward the grid and coated onto CuO NWs on the TEM grid.

■ RESULTS AND DISCUSSION

Surface Functionalization of CuO NWs with SnO$_2$ NCs. The oxidation of copper at 450 °C resulted in a top layer of high-density crystalline CuO NWs on the Cu foil, which is consistent with our prior results.[20,27,30] Some as-grown NWs were transferred onto a nickel grid for SEM and TEM characterizations. Figure 1a is a representative SEM image of synthesized CuO NWs, whose diameters range from tens of nm

to a few hundred nm and lengths are over several μm. All the NWs showed clean and smooth surfaces. In our previous work, we confirmed the crystallinity of as-grown CuO NWs using X-ray diffraction (XRD) and HRTEM.[20,27,30]

Aerosol SnO$_2$ NCs were synthesized using an arc plasma source.[28,29] Our detailed characterizations of thus-produced SnO$_2$ NCs have revealed their rutile crystalline structure. We used the ESFDA process[21,22] to deposit SnO$_2$ NCs onto CuO NWs. Figure 1b shows some CuO NWs after 3-min deposition of SnO$_2$ NCs. Unlike the bare CuO NWs (Figure 1a), particlelike entities are clearly seen on CuO NWs in Figure 1b, indicating the successful assembly of SnO$_2$ NCs onto CuO NWs. The NCs distributed on NWs quite uniformly without agglomeration, which is consistent with our previous results obtained using the ESFDA process.[21,22] For 3 min NC deposition, the NWs were not entirely covered with NCs and they still had plenty of open surface area to interact with gas molecules.

We obtained more convincing evidence for depositing SnO$_2$ NCs onto CuO NWs by TEM observation of the same CuO NWs before and after the NC assembly. More details about this location-tracking procedure coupled with TEM and HRTEM imaging of nanomaterials can be found in our previous studies.[31−33] Figure 1c is a TEM image of a single CuO NW, which has a diameter of ∼60 nm and smooth surface, consistent with the SEM observation (Figure 1a). Figure 1e is an HRTEM image of the same NW shown in Figure 1c. The fringes in the HRTEM image (Figure 1e) evidently confirm the crystalline nature of the CuO NW, agreeing with our previous results[20,27,30] and those from other groups.[26] Lattice spacing analysis by numerical diffractograms reveals a value of 0.274 nm, corresponding with the (110) plane of CuO.

This same CuO NW was imaged again in TEM after depositing SnO$_2$ NCs for 3 min. As shown in Figure 1d, many NCs with sizes mostly less than 10 nm are clearly seen on the NW surface. The NCs distributed on the NW surface quite uniformly and no agglomerated NCs were seen on the NW, which agrees with the SEM observation. In the HRTEM image of Figure 1f, we see fringes not only from the CuO NW (0.274 nm) but also from the SnO$_2$ NC (0.336 nm). The lattice spacing of 0.336 from the NC corresponds with the (110) plane of rutile SnO$_2$, which agrees with our previous results.[28,29] A sample after 10 min of ESFDA process was found to have a nearly continuous layer of SnO$_2$ NCs on CuO NWs (see Figure S1 in the Supporting Information).

In Figure 1f, a thin layer of amorphous carbon is seen between the CuO NW and the SnO$_2$ NC. This layer could be formed during TEM characterization of the bare CuO NWs when Figure 1c and 1e were obtained. It has been commonly observed that amorphous carbon can be deposited onto a sample when electron beam interacts with residue hydrocarbons inside a TEM.[34] We prepared a fresh sample of CuO NWs coated with SnO$_2$ NCs (i.e., the bare NWs were not imaged using TEM before SnO$_2$ NC deposition) and found that the interface between the NWs and NCs was clean (i.e., the NWs and NCs were in good contact). A representative HRTEM image of this sample is shown in Figure S2 in the Supporting Information.

We previously investigated the binding mechanism for the structure of CNTs coated with NCs.[31] The NC−CNT structure was produced by the same processes used in this study (i.e., NCs from the arc plasma reactor; NCs assembly using the ESFDA process). Our experimental and theoretical
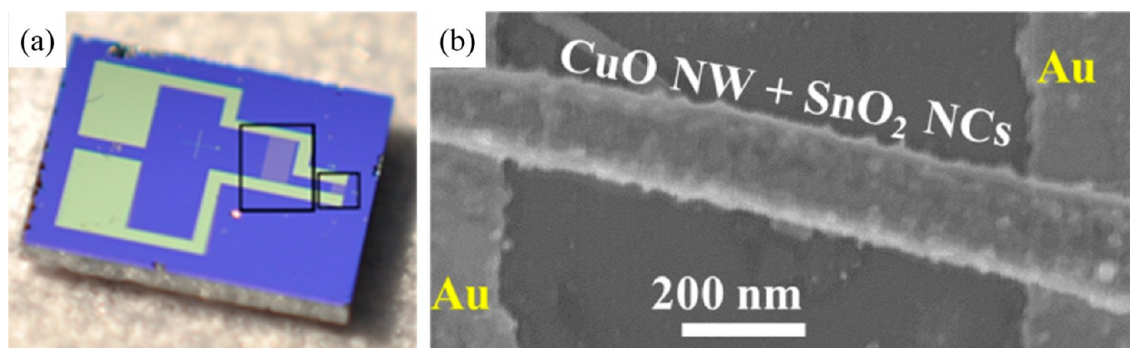
4194

dx.doi.org/10.1021/am300911z | ACS Appl. Mater. Interfaces 2012, 4, 4192−4199

Figure 2. (a) Photo of an Si chip (∼4 × 5 mm^2) with Au interdigitated electrodes (boxed areas). (b) SEM image of an SnO$_2$ NC-functionalized CuO NW bridging a pair of Au fingers.
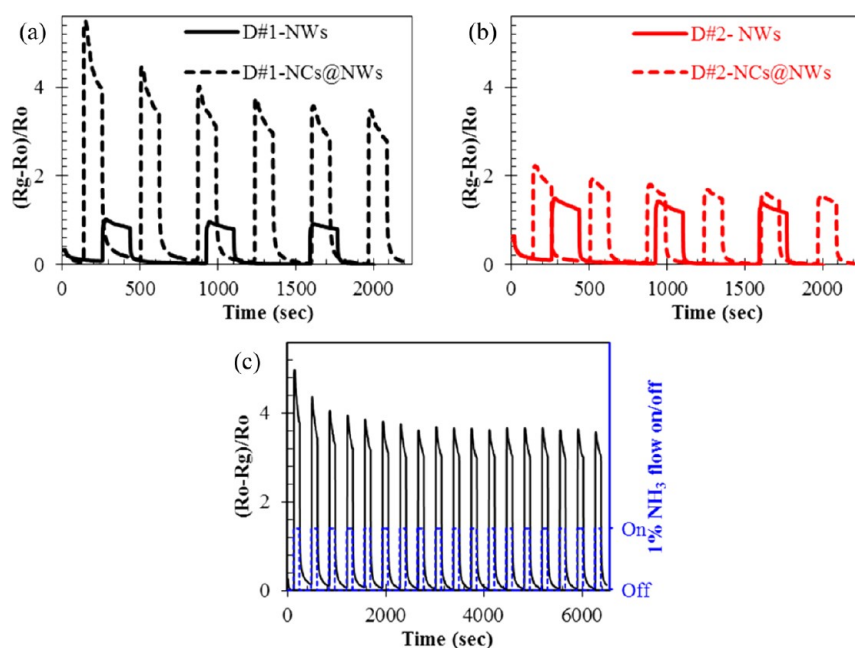

Figure 3. Dynamic responses of Devices (a) 1 (D#1) and (b) 2 (D#2) to 1% NH$_3$ at room temperature. Both devices showed improved sensitivity after surface functionalization with SnO$_2$ NCs (3 min for D#1 and 6 min for D#2), clearly indicated by the sharp contrast between the dashed curve (CuO NWs coated with SnO$_2$ NCs) and the solid curve (bare CuO NWs) of the same color. (c) Eighteen cycles of 1% NH$_3$ detection using D#1-NCs@NWs. Each cycle consists of, sequentially, 2 min of clean air flow, 2 min of 1% NH$_3$ flow (diluted in air), and 2 min of clean air for sensor recovery. D#1-NCs@NWs displaced mostly repeatable sensing signal and excellent dynamic properties (i.e., instantaneous response upon NH$_3$ exposure and rapid recovery in air). (Note that NCs@NWs stands for NWs coated with NCs.).

data suggested that NCs are attached to CNTs through van der Waals force and the binding is strong enough to hold NCs on CNTs. Considering that the same methods were used for NCs synthesis and assembly, NCs could be bound to CuO NWs through van der Waals force and remain on NWs quite stably.

Sensing Devices Fabricated. Figure 2a shows an Si chip (∼ 4 × 5 mm^2) with Au interdigitated electrodes being highlighted in the two black boxes. The two large Au contact pads and associated thick Au wires on the chip were fabricated using photolithography, whereas interdigitated electrodes (or fingers) with both width and interspacing of ∼1 μm were fabricated by e-beam lithography. Prefabrication of electrodes in the absence of NWs prevents NWs from contamination by photoresists used in photolithography and e-beam lithography.

CuO NW sensors were made by drop-casting NWs suspension (methanol as solvent) onto an Si chip with Au interdigitated electrodes. After the methanol evaporation, a sparse network of CuO NWs was left on the electrode,

spanning across neighboring fingers and thereby closing the sensor circuit. The number density of NWs on the electrode was about 0.1 NW/μm^2 (see Figure S3 in the Supporting Information), resulting in approximately 10,000 NW/device. Methanol was chosen to disperse CuO NWs, because it easily evaporates and requires no additional surfactant that could potentially modify NW surfaces. The coverage density of NWs on the interdigitated electrode could be varied by simply adjusting the concentration of the CuO NW-methanol suspension. As-fabricated CuO NW devices were further annealed in an Ar flow at 200 °C for one hour to remove remnant methanol on NWs and on chips. This annealing step also improved the NW-Au contact. Our previous work suggested that the contact between CuO NWs and metal electrode is Ohmic, since symmetric and linear drain-source I_{ds}−V_{ds} curves were observed.[20] Additionally, Liao et al. reported that Ohmic contact can be formed between CuO NWs and Au electrodes.[35] The role of the NW-electrode

contact during gas detection is still open for debate and further efforts are needed to investigate the influence of the contact on the sensing performance of NW sensors.

Although we were not able to make single NW-based devices as before,[20] our current procedure has the advantage of keeping the NW "clean" during the course of the device fabrication. Indeed, compared with single NW devices (which could be contaminated by photo resist), the networks of CuO NWs with clean surfaces showed much improved sensing response (to be discussed). Devices with SnO_2 NC-functionalized CuO NWs were obtained by assembling SnO_2 NCs onto CuO NWs using the ESFDA process. Figure 2b is a representative SEM image from a CuO NW device with 3-min SnO_2 NC deposition. One can clearly see SnO_2 NCs decorating on the surface of a CuO NW that bridges a pair of neighboring Au fingers. It seems unlikely that the nature of the contact between CuO NWs and Au electrodes could be affected by the deposition of SnO_2 NCs, because the NW-electrode contact was formed before the ESFDA process. However, further study is required if one wants to rule out the possible influence of NCs on the NW-electrode contact.

Sensing with CuO NWs and SnO_2 NC-Functionalized CuO NWs. The dynamic responses (sensitivity vs time) of two sensors, Device 1 (D#1) and Device 2 (D#2), for detecting 1% NH_3 diluted in air are shown in Figure 3a and 3b, respectively. The sensor sensitivity is evaluated as the ratio of $(R_g - R_o)/R_o$, where R_o is the sensor resistance in air and R_g is the sensor resistance in the challenging gas. For bare CuO NW devices, three cycles were repeated for both devices (denoted as D#1-NWs and D#2-NWs), as shown by the solid curves (black for D#1-NWs and red for D#2-NWs) in panels a and b in Figure 3, respectively; the sensing behavior appeared fairly reproducible.

Upon exposure to 1% NH_3 gas, D#1-NWs and D#2-NWs both exhibited instantaneous responses as their resistances increased rapidly, resulting in sensitivities greater than 0. Instead of a monotonic increase in sensitivity typically observed during the NH_3 exposure, the sensitivity of D#1-NWs and D#2-NWs first rapidly reached a maximum value and then slowly decayed. Similar behavior has been reported in detecting NH_3 using nanostructures, such as a nanojunction created within a silver NW,[36] tungsten oxide NW films,[37] and vertically aligned silicon NWs;[38] however, the origin of this peculiarity in NH_3 sensing (i.e., sensitivity increases first and then decays) is yet to be understood. The sensing signal quickly returned to the baseline after NH_3 was turned off and clean dry air was restored. With bare CuO NWs, D#1-NWs had a sensitivity of ~0.92 (solid black curve in Figure 3a), a response time of ~9 s, and a recovery time of ~6 s; D#2-NWs had a sensitivity of ~1.5 (red solid curve in Figure 3a), a response time of ~4.5 s, and a recovery time of ~6 s. (Note that the response time or recovery time is defined as the time needed to reach 90% of change between the initial and final equilibrium values.) The NH_3 sensing performance of D#1-NWs and D#2-NWs noticeably exceeded that of our single CuO NW-based sensors (with the sensitivity of ~0.06; the response time and recovery time of ~40 s and ~8 min, respectively).[20] The improved room-temperature sensing properties of D#1-NWs and D#2-NWs could be mainly attributed to our efforts of keeping the surfaces of CuO NWs from photoresist contamination during the device fabrication. In addition, other factors, such as the good contact between NWs and Au electrode (improved by annealing in Ar at 200 °C) and the large surface area of the NWs, could have

also helped enhance the sensing performance of our CuO NW devices at room temperature.

The sensitivity of D#1-NWs and D#2-NWs for NH_3 is also higher than CuO NW sensors reported in the literature. For example, the sensors based on CuO NW arrays were found to have a sensitivity of ~0.15, a response time of ~125 s, and a recovery time of ~500 s for 0.5% NH_3 when operating at 160 °C;[18] a projected sensitivity of these NW array sensors is ~0.3 for 1% NH_3, if a linear relation is assumed between the sensitivity and the NH_3 concentration. D#1-NWs and D#2-NWs exhibited not only higher NH_3 sensitivity (~ 0.9 and 1.5, respectively), but also attractive dynamic properties even running at room temperature. This room-temperature operation can simplify sensor design and save energy as heating elements can be eliminated.

It is generally accepted that surface defects of metal oxides act as O_2 adsorption sites.[39] Considerable oxygen adsorption occurs on CuO surface at temperatures as low as 10 °C.[40] The O_2 molecules adsorbed at surface defect sites serve as electron acceptors in the chemisorption process, leading to negatively charged oxygen adsorbates (e.g., O^- or O_2^-) at the metal oxide surface via reactions such as: $O_2 + 2e^- \rightarrow 2O^-$ and $O_2 + e^- \rightarrow O_2^-$. The presence of these oxygen adsorbates results in a local accumulation of holes near the surface of the p-type CuO NW, thereby increasing the NW conductivity. In the presence of NH_3 (a reducing gas, i.e., an electron donor), the oxygen adsorbates (e.g., O^-) have been previously found to react with NH_3 in accordance with the following reaction: $2NH_3 + 3O^- \rightarrow 3H_2O + N_2 + 3e^-$.[41] Therefore, the electron transfer from NH_3 to the CuO NW decreases the hole concentration in the NW, thereby increasing its resistance.[9,19,42]

SnO_2 NCs were assembled onto CuO NWs in both D#1-NWs and D#2-NWs with NC deposition times of 3 and 6 min, respectively. (Note that NCs should not fully cover a NW as the deposition time is less than 10 min) After surface functionalization with SnO_2 NCs, both sensors (denoted as D#1-NCs@NWs and D#2-NCs@NWs) displayed strikingly improved responses to 1% NH_3, as clearly indicated by the two dashed curves (black for D#1-NCs@NWs and red for D#2-NCs@NWs) in panels a and b in Figure 3. With SnO_2 modification, D#1-NCs@NWs and D#2-NCs@NWs had average sensitivities of ~4 and ~1.8, respectively, response times of ~9 and ~10 s, respectively, and recovery times of both ~6 s. Specifically, D#1 improved its NH_3 sensitivity by ~300% and D #2 enhanced its sensitivity by ~20%. In addition, the sensing signals of these SnO_2 NC-functionalized CuO sensors were quite repeatable, as shown in Figure 3c, where 18 cycles were plotted for 1% NH_3 detection using D#1-NCs@NWs. Except for the first few cycles, the sensitivity was fairly reproducible without drifting. Clearly, functionalization of CuO NWs with SnO_2 NCs leads to pronounced increment in NH_3 sensitivity while imposing no detrimental effects on the dynamic properties of the sensors.

Interestingly, before SnO_2 NC functionalization, D#2-NWs had higher sensitivity than D#1-NWs (1.5 vs 0.9); however, D#2 with 6-min SnO_2 NC deposition only had a relatively modest improvement in sensitivity (~ 20%), while D#1 with 3-min SnO_2 NC coating achieved an ~300% increase in sensitivity. Our speculation is that higher coverage of SnO_2 NCs on CuO NWs may not further improve sensing performance; instead, there could be a critical NC number density for optimum modification of CuO NWs. Further study is needed to investigate the detailed relation between the NC
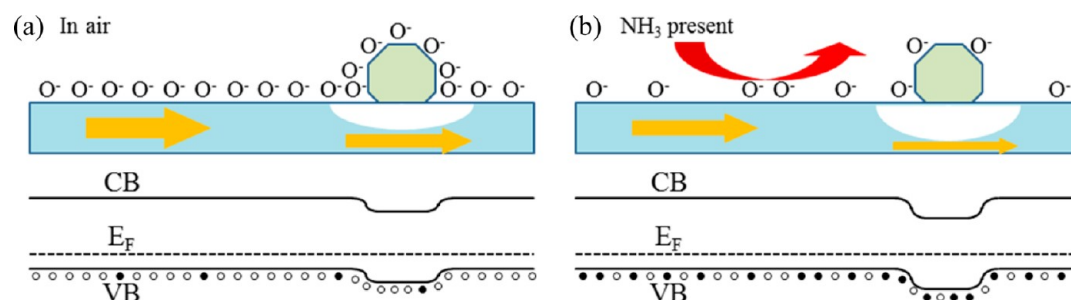
Figure 4. Schematics and band diagrams of the SnO_2 NC-CuO NW structure (a) before and (b) after it is exposed to NH_3 gas. (●, electron; ○, hole).
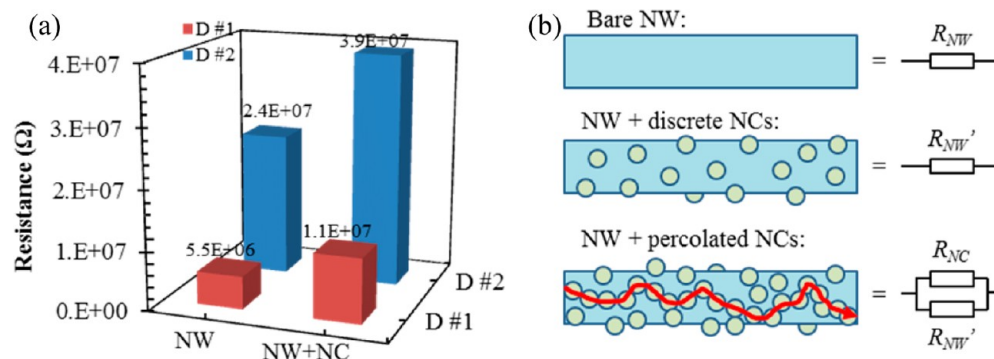

Figure 5. (a) Resistances of D #1 and D #2 both increased after SnO_2 NC deposition, implying the formation of p−n junctions between SnO_2 NCs and CuO NWs. (b) Schematics showing the influence of NC number density on the resistance of the SnO_2 NC-CuO NW structure. Coverage with discrete NCs increases the NW resistance from R_{NW} to R_{NW}' due to p−n junctions; higher NC coverage leads to percolation between adjacent NCs, and percolated NCs causes a resistance R_{NC} in parallel with R_{NW}'.

number density and the sensing improvement of the NC-NW structure.

Proposed Sensing Mechanism for the NC-NW Structure. The p−n junction formed between the p-type CuO NW and the n-type SnO_2 NC can play a vital role in modulating the sensing behavior of the NC-NW devices (as presented in Figure 3a). In Figure 4, we proposed a simplified model to shed light on the sensing behavior of the NC-NW structure. In air (Figure 4a), the CuO NW and SnO_2 NC are both covered with negatively charged oxygen ions (O^-) because of the oxygen adsorption on the metal oxides. These oxygen adsorbates draw electrons from the metal oxides, making p-type CuO more conductive (increased hole concentration) and n-type SnO_2 more resistive (lowered electron concentration). In addition, the formation of a p−n junction between the CuO NW and the SnO_2 NC not only locally lowers hole concentration in the NW but also creates a barrier for holes to transport in the valence band of the CuO NW, both locally lowering the conductance of the NW. Upon exposure to NH_3 (electron donor), the density of oxygen adsorbates on CuO and SnO_2 surfaces decreases along with electrons transferring from NH_3 to the CuO NW and SnO_2 NC (Figure 4b). Only one CuO NW was considered in our model, while a network of NWs was actually present in a real device that we fabricated. A more sophisticated model is thus needed in the future to help understand the NC-NW system with improved reliability. This new model should take into account of more factors, such as the number density of NWs in a device, and the NW-to-NW junctions in a network.

The surface area of a CuO NW coated with SnO_2 NCs is indeed higher than that of the bare NW. This enhanced surface area of the NC-NW structure leads to more adsorption sites for gaseous molecules, which could help improve the sensing performance of the NC-NW structure. However, the CuO NW is the signal transducing channel in the NC-NW system (particularly for discrete NCs on NWs) and the NCs still have to interact with the NW for the target gaseous molecules adsorbed on NCs to be sensed. Additionally, D#2-NCs@NWs had higher coverage of NCs (6 min NC deposition) than D#1-NCs@NWs (3 min NC deposition); however, the NH_3 sensitivity of D#2-NCs@NWs is lower than that of D#1-NCs@NWs. We thus speculate that the p−n junction formed between SnO_2 NCs and CuO NWs plays a more important role than the surface area in the NC-NW sensing system. In fact, other researchers[43,44] have previously suggested the formation of p−n junction between SnO_2 and CuO and used it as sensing mechanism to explain the observed gas sensing behavior. It is worth noting that our NC-NW structure (CuO NWs coated with SnO_2 NCs) is different from those formerly reported structures (SnO_2 NWs[43] or films[44] coated with CuO NCs). Moreover, our NC-NW sensors showed excellent room temperature sensing performance, whereas previous studies[43,44] characterized their sensors only at elevated temperatures.

In contrast to bare CuO NWs, two factors should be considered for the enhanced sensitivity of CuO NWs functionalized with discrete SnO_2 NCs: (1) the hole concentration in the CuO NW is lowered because of electron transfer from NH_3 to the CuO NW, thereby increasing the NW resistance; (2) higher electron concentration in the SnO_2 NC because of lowered coverage of oxygen adsorbates could render a stronger p−n junction, which could further block the local hole transport around the junction region in the CuO NW and increase the NW resistance.

These two factors jointly influence the sensing process for the SnO_2 NC-CuO NW system, and their combined effect could depend on the NC coverage. For a CuO NW with discrete SnO_2 coverage, both factors could be important for the sensing. Increased NC coverage can complicate the NC-NW system as conducting paths form among neighboring NCs. A CuO NW will eventually lose direct interaction with NH_3 if a continuous layer of SnO_2 NCs is deposited on it, leaving only the second factor effective. Additional experimental and theoretical studies are needed to fully understand the NC-NW system and to identify the most dominant factor under different gaseous environment and with varying NC coverage.

D#1 and D#2 showed increased resistances with deposition of SnO_2 NCs (Figure 5a), implying the formation of p−n junctions between NCs and NWs and thereby supporting the model proposed in Figure 4. However, with 3-min NC deposition, D#1 doubled its resistance (from 5.5×10^6 Ω to 1.1×10^7 Ω); but D#2 only increased its resistance by ~60% (from 2.4×10^7 Ω to 3.9×10^7 Ω) even with longer-time NC deposition (6 min). This suggests that the SnO_2 NC coverage on the CuO NW also affects the overall resistance of the NC-NW structure, in addition to the interaction between the NCs and NW (i.e., increase in resistance due to p−n junctions). As shown in Figure 5b, discrete NCs on a NW by a short duration of NC deposition increase the NW resistance from R_{NW} to R_{NW}' due to the p−n junction formation. On the other hand, higher coverage of NCs will cause percolation of NCs, resulting in conducting path(s) in NCs (the red arrowed curve in Figure 5b). Percolated NCs can act as a resistor (R_{NC}) in the NC-NW system. Although R_{NC} could be much larger than R_{NW}' (because of small sizes of NCs and the numerous grain boundaries in an NC conducting path), R_{NC} could still counteract the p−n junction induced resistance increase as it is in parallel with R_{NW}'. In addition, for NH_3 sensing, R_{NC} decreases as electrons transfer from NH_3 to SnO_2 NCs, offsetting the sensing signal due to the increase in R_{NW}'. Indeed, we observed that D #2 (with 6-min SnO_2 NC deposition) only increased its NH_3 sensitivity by ~20% and that D #1 (with 3 min SnO_2 NC coating) almost tripled its sensitivity. Our experimental observations here suggest that the NC coverage on the NW could be used to adjust the sensing properties of the NC-NW structure. Further characterizations (e.g., current (I_{ds}) versus gate voltage (V_g) tests) could provide additional information to better understand properties of the NC-NW system, which will be used in our future study.

CONCLUSION

We have demonstrated that CuO NWs surface functionalized with SnO_2 NCs can have better performance for room-temperature gas sensing. The improved sensitivity could be attributed to the creation of p−n junctions between the host p-type CuO NW and deposited n-type SnO_2 NCs. The operating temperature for the SnO_2 NC-CuO NW sensing system is as low as room temperature, in contrast to the required high temperature (typically above 200 °C) for SnO_2 NW-based sensors. Moreover, the differential sensitivity between CuO NWs and SnO_2 NCs, the coverage of SnO_2 NCs on CuO NWs (or number density of NCs on NWs), and doping of SnO_2 NCs offer tremendous flexibility in modulating the sensing performance of CuO NW sensors, which holds promise for engineering the selectivity of gas sensors.

ASSOCIATED CONTENT

S Supporting Information
Figures S1, S2, and S3. This material is available free of charge via the Internet at http://pubs.acs.org.

AUTHOR INFORMATION

Corresponding Author
*E-mails: ganhualu@uwm.edu; jhchen@uwm.edu.

Notes
The authors declare no competing financial interest.

REFERENCES

(1) Lieber, C. M.; Wang, Z. L. *MRS Bull.* **2007**, *32*, 99−108.
(2) Cui, Y.; Wei, Q. Q.; Park, H. K.; Lieber, C. M. *Science* **2001**, *293*, 1289−1292.
(3) Shen, G.; Chen, P. C.; Ryu, K.; Zhou, C. *J. Mater. Chem.* **2009**, *19*, 828−839.
(4) Kong, J.; Franklin, N. R.; Zhou, C. W.; Chapline, M. G.; Peng, S.; Cho, K. J.; Dai, H. J. *Science* **2000**, *287*, 622−625.
(5) Kauffman, D. R.; Star, A. *Angew. Chem., Int. Ed.* **2008**, *47*, 6550−6570.
(6) Cao, Q.; Rogers, J. A. *Adv. Mater.* **2009**, *21*, 29−53.
(7) Collins, P. G.; Bradley, K.; Ishigami, M.; Zettl, A. *Science* **2000**, *287*, 1801−1804.
(8) Kolmakov, A.; Klenov, D. O.; Lilach, Y.; Stemmer, S.; Moskovits, M. *Nano Lett.* **2005**, *5*, 667−673.
(9) Gou, X. L.; Wang, G. X.; Yang, J. S.; Park, J.; Wexler, D. *J. Mater. Chem.* **2008**, *18*, 965−969.
(10) Kuang, Q.; Lao, C.-S.; Li, Z.; Liu, Y.-Z.; Xie, Z.-X.; Zheng, L.-S.; Wang, Z. L. *J. Phys. Chem. C* **2008**, *112*, 11539−11544.
(11) Kauffman, D. R.; Star, A. *Nano Lett.* **2007**, *7*, 1863−1868.
(12) Kong, J.; Chapline, M. G.; Dai, H. J. *Adv. Mater.* **2001**, *13*, 1384−1386.
(13) Sun, Y. G.; Wang, H. H. *Adv. Mater.* **2007**, *19*, 2818−2823.
(14) Collins, B. T.; Desisto, W.; Kershaw, R.; Dwight, K.; Wold, A. *J. Less-Common Met.* **1989**, *156*, 341−346.
(15) Ito, T.; Yamaguchi, H.; Masumi, T.; Adachi, S. *J. Phys. Soc. Jpn.* **1998**, *67*, 3304−3309.
(16) Nakamura, Y.; Yoshioka, H.; Miyayama, M.; Yanagida, H.; Tsurutani, T.; Nakamura, Y. *J. Electrochem. Soc.* **1990**, *137*, 940−943.
(17) Jung, S. J.; Yanagida, H. *Sens. Actuators, B* **1996**, *37*, 55−60.
(18) Chen, J. J.; Wang, K.; Hartman, L.; Zhou, W. L. *J. Phys. Chem. C* **2008**, *112*, 16017−16021.
(19) Li, D. D.; Hu, J.; Wu, R. Q.; Lu, J. G. *Nanotechnology* **2010**, *21*.
(20) Hansen, B. J.; Kouklin, N.; Lu, G. H.; Lin, I. K.; Chen, J. H.; Zhang, X. *J. Phys. Chem. C* **2010**, *114*, 2440−2447.
(21) Chen, J. H.; Lu, G. H. *Nanotechnology* **2006**, *17*, 2891−2894.
(22) Lu, G. H.; Zhu, L. Y.; Wang, P. X.; Chen, J. H.; Dikin, D. A.; Ruoff, R. S.; Yu, Y.; Ren, Z. F. *J. Phys. Chem. C* **2007**, *111*, 17919−17922.
(23) Lu, G. H.; Ocola, L. E.; Chen, J. H. *Adv. Mater.* **2009**, *21*, 2487−2491.

(24) Streetman, B. G., *Solid State Electronic Devices*, 4th ed.; Prentice Hall: Englewood Cliffs, NJ, 1995.

(25) Williams, D. E., *Conduction and Gas Response of Semiconductor Gas Sensors*; Adam Hilger: Bristol, U.K., 1987.

(26) Jiang, X. C.; Herricks, T.; Xia, Y. N. *Nano Lett.* **2002**, *2*, 1333−1338.

(27) Hansen, B. J.; Lu, G. H.; Chen, J. H. *J. Nanomater.* **2008**, 830474.

(28) Chen, J. H.; Lu, G. H.; Zhu, L. Y.; Flagan, R. C. *J. Nanopart. Res.* **2007**, *9*, 203−213.

(29) Cui, S.; Mattson, E.; Lu, G.; Hirschmugl, C.; Gajdardziska-Josifovska, M.; Chen, J. *J. Nanopart. Res.* **2012**, *14*, 1−13.

(30) Hansen, B. J.; Chan, H. L.; Lu, J. A.; Lu, G. H.; Chen, J. H. *Chem. Phys. Lett.* **2011**, *504*, 41−45.

(31) Zhu, L. Y.; Lu, G. H.; Mao, S.; Chen, J. H.; Dikin, D. A.; Chen, X. Q.; Ruoff, R. S. *Nano* **2007**, *2*, 149−156.

(32) Lu, G. H.; Mao, S.; Park, S.; Ruoff, R. S.; Chen, J. H. *Nano Res.* **2009**, *2*, 192−200.

(33) Yu, K. H.; Lu, G. H.; Bo, Z.; Mao, S.; Chen, J. H. *J. Phys. Chem. Lett.* **2011**, 1556−1562.

(34) Williams, D. B.; Carter, C. B., *Transmission Electron Microscopy: A Textbook for Materials Science*, 2nd ed.; Springer: New York, 2009.

(35) Liao, L.; Zhang, Z.; Yan, B.; Zheng, Z.; Bao, Q. L.; Wu, T.; Li, C. M.; Shen, Z. X.; Zhang, J. X.; Gong, H.; et al. *Nanotechnology* **2009**, *20*, 085203.

(36) Xing, W. D.; Hu, J.; Kung, S. C.; Donavan, K. C.; Yan, W. B.; Wu, R. Q.; Penner, R. M. *Nano Lett.* **2012**, *12*, 1729−1735.

(37) Zhao, Y. M.; Zhu, Y. Q. *Sens. Actuators, B* **2009**, *137*, 27−31.

(38) Field, C. R.; In, H. J.; Begue, N. J.; Pehrsson, P. E. *Anal. Chem.* **2011**, *83*, 4724−4728.

(39) Batzill, M.; Diebold, U. *Prog. Surf. Sci.* **2005**, *79*, 47−154.

(40) Iwamoto, M.; Yoda, Y.; Yamazoe, N.; Seiyama, T. *J. Phys. Chem.* **1978**, *82*, 2564−2570.

(41) Wagh, M. S.; Jain, G. H.; Patil, D. R.; Patil, S. A.; Patil, L. A. *Sens. Actuators, B* **2006**, *115*, 128−133.

(42) Wang, C.; Fu, X. Q.; Xue, X. Y.; Wang, Y. G.; Wang, T. H. *Nanotechnology* **2007**, 18.

(43) Hwang, I.-S.; Choi, J.-K.; Kim, S.-J.; Dong, K.-Y.; Kwon, J.-H.; Ju, B.-K.; Lee, J.-H. *Sens. Actuators, B* **2009**, *142*, 105−110.

(44) Chowdhuri, A.; Sharma, P.; Gupta, V.; Sreenivas, K.; Rao, K. V. *J. Appl. Phys.* **2002**, *92*, 2172−2180.